Appendix 1. Climate suitability models, ensemble forecast and their performances

Niche models

We performed the projections using 9 different widely used niche-based modelling techniques among which 8 were performed with the BIOMOD computational framework (Thuiller 2003): (1) generalized linear model (GLM), a regression method with polynomial terms for which a stepwise procedure is used to select the most significant variables, (2) generalized additive model (GAM), another regression method with 4 degrees of freedom and a stepwise procedure to select the most parsimonious model, (3) classification tree analysis (CTA; Breiman *et al*. 1984), a classification method running a 50-fold cross-validation to select the best trade-off between the number of leaves of the tree and the explained deviance, (4) artificial neural networks (ANN; Ripley 1996), a machine learning method, with the mean of 3 runs used to provide predictions and projections, as each simulation gives slightly different results, (5) mixture discriminant analysis (MDA; Hastie & Tibshirani 1996), a classification method based on mixture models, (6) multivariate adaptive regression splines (MARS; Friedman 1991), a nonparametric regression method mixing CTA and GAM, which could be viewed as an ancestor of GBM, (7) generalized boosting model (GBM; Ridgeway 1999), a machine learning method which combines a boosting algorithm and a regression tree algorithm to construct an 'ensemble' of trees, and (8) Random Forest (RF; Breiman 2001), a machine learning method which is a combination of tree predictors such that each tree depends on the values of a random vector sampled independently and with the same distribution for all trees in the forest. Finally, we run (9) Maxent version 3 (Phillips *et al.* 2006), a machine learning method that estimates species distributions by finding the distribution of maximum entropy subject to the constraint that the expected value of each environmental variable under this estimated distribution matches its empirical average. All models used in this study need information about presences and absences to be able to determine suitable conditions for a given species. As our dataset contained only presence data, we needed to define pseudo-absences (see Appendix 2).

Independant validation of species models

In order to assess the accuracy of our final distributions, we provide independent validations of individual species' models, by using the wintering distribution maps from the Handbooks of "The Birds of Africa" (Keith & Fry 1992-2004). Presence/absence data was obtained by digitizing the maps with ArcGis 9.1. The AUC calculated with this independent set of data

ranges from 0.72 to 0.99 (0.92±0.06, Appendix 3). Generally, models with AUC>0.9 are considered to perform very well, and values of AUC>0.7 are considered as acceptable (Swets 1988). Therefore, the models and its consensus seem robust and predictive, so the climate forecasts can be applied for all species.

Consensus maps

For each species and each climate model, the selection of the 5 best models for the consensus method was based on ROC curves and the Area Under Curve criteria (AUC; Fielding & Bell 1997). Regarding the ensemble forecast technique, we tested two ways of using the selected models, by calculating either the weighted mean (with AUC as weights, as described in Marmion *et al*. 2008) or the unweighted mean. The present distributions we obtain did not show any differences as for their centroids (paired t-test for the latitude: t=-0.773, df=63, p=0.44; paired t-test for the longitude: t=1.269, df=63, p=0.21). There was a significant difference between range sizes obtained from both methods (paired t-test: t=5.349, df=63, p<0.001), but this difference was small (ranging from -2.0% to +3.9%). In order to minimize potential flaws resulting from the wide use of AUC values (see Lobo et al. 2008), we decided to use unweighted means here.

AUC use and limits

According to Lobo et al. (2008), the AUC technique is not recommended to assess the accuracy of predictive distribution models, mainly because it varies with parameters such as the prevalence, the number of pseudo-absences and the total extent to which models are carried out, which do not occur here because we use AUC to compare different models obtained for one species, using the same presences and pseudo-absences data, across the same geographical area. (1) AUC can be biased by variations in pseudo-absence selection, but in our study, pseudo-absences were selected with a similar procedure for all species, and most importantly, for a given species, the same set of randomly-selected pseudo-absences was used for running the different modelling techniques. (2) AUC varies with the total extent to which models are carried out, as it influences the rate of well-predicted absences. This is the most important flaw cited by Lobo et al. (2008). In this study, the extent area where models are performed is fixed, so this major limitation does not apply in this case. (3) AUC weights omission and commission errors equally. From a reserve-design point of view, misclassifications of absences (commission errors) must be regarded as a more serious drawback than the opposite; on the other hand, low omission errors are desirable when

searching for new species or populations. In the case of simply modelling probabilistic distributions, with the aim of comparing distributions obtained with the same presence – absence data for a species, weighting omission and commission equally should not produce bias able to discredit the comparison. (4) Finally, pseudo-absences have a higher degree of uncertainty than presences, because they are selected randomly within absence areas which may be due, simply, to low detectability of the species, or may correspond to non-sampled areas. Because of this, false absences are more likely to occur than false presences and, consequently, commission errors should not weigh as much as omission errors. To deal with this, we decided to select the pseudo-absences outside the area predicted as suitable by the SRE model, in order to minimize the probability of false absences (see Appendix 2). Defining also a total sample size (presences and pseudo-absences) similar for all species also helped facing this problem. A species with a restricted number of presence records is likely absent from most of the rest of Africa, so that a high number of pseudo-absences can be considered realistic. On the opposite, a species with widespread numerous presence records (e.g. Swallow, Yellow Wagtail) are likely present in most of Africa, and a low number of pseudo-absences should minimize the creation of false absence data.

Lastly, according to Lobo et al. (2008), accuracy measures proposed in the literature can be used to compare techniques for the same species at the same extent. In this case, instead of using only the AUC, they propose that sensitivity and specificity should be also reported, so that the relative importance of commission and omission errors can be considered to assess the method performance. The authors said they cannot recommend any useful method to compare model performance among species. For the purpose of producing consensus maps by comparing models obtained for a given species at a fixed spatial scale, we are clearly falling within these cases, and we report sensitivity and specificity to Appendix 3.

Variations among models, scenarios, sample size

In order to study the relative performances of the different niche modelling techniques, we considered AUC calculated from the modelled present winter ranges. AUC values varied significantly between niche modelling techniques, with RF and GBM being the best performing models, followed by GAM and ANN, and GLM (Fig. S1). The mean performance of all models is good, with only a few cases with AUC values below 0.7.

Figure S1. Box plot of AUC values obtained for all present predictions according to the climate suitability model used. Median, first and third quartiles, lower and upper adjacent limits are depicted, as well as outlying values. n = 320 AUC values per model, obtained by predictions for 64 species with each of the 5 GCMs.

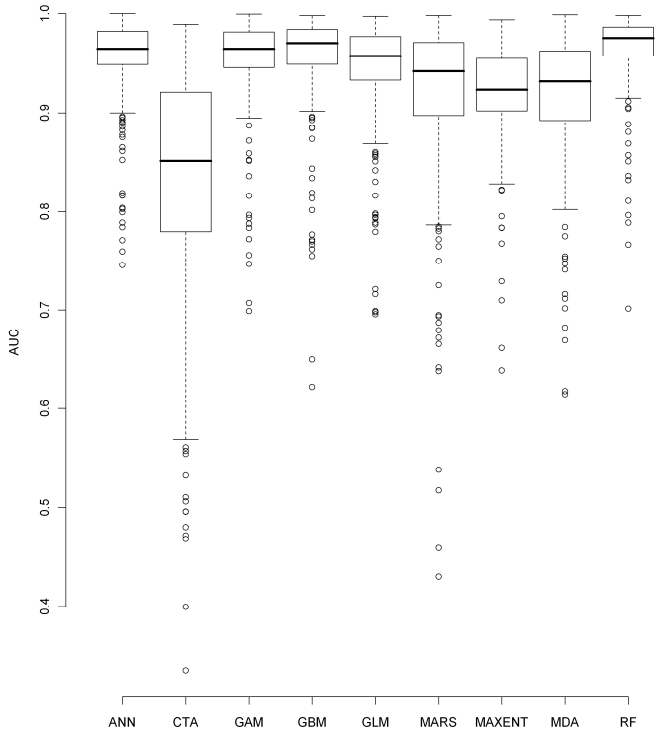

Figure S2 reports on the frequency a niche modelling technique was chosen by the consensus method, and confirms that RF, GBM, GAM, ANN and GLM are the 5 best performing models, used in more than 75% of the ensemble forecasts. Figure S3 shows the mean AUC according to the niche modelling technique and to the number of presence data available per species. Even though the comparison of AUC between species could arise some problems (Lobo et al. 2008) the gathering of species with close number of presence data eliminates most of the flaws and can bring some information. This underlines that the models behave in different ways according to the number of data. For example, the relative bad

performance of the CTA model seems to be due to a bad performance for species with less than 200 presence data. Moreover, this figure shows that for the species for which less than 20 presence data were available, there are always at least 5 techniques with a mean AUC over 0.85, making it possible to keep species with down to 6 occurrence points. Besides, the low performance of a few models when too few presence data was available further justified, if needed, the choice for a consensus method that excluded, for each species and each climate scenario, the 4 least performing models.

When observing the distribution of the ratio of range sizes (log-transformed) for each of the 9 models (Figure S4), it appears that the ANN model predicted smaller variations in winter ranges (smaller standard deviation with the same mean).

Figure S2. Frequency and selection rank of the climate suitability model that have been selected by the concensus method

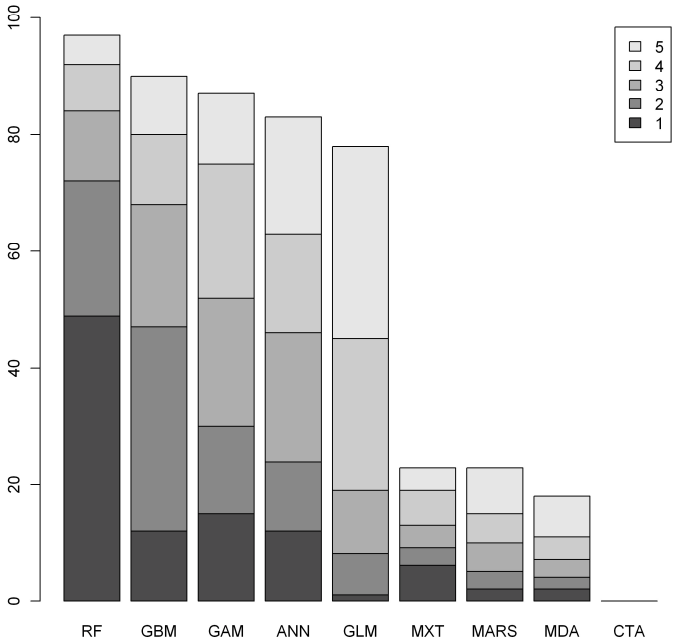

Figure S3. Means of the AUC values obtained for each climate suitability model according to the number of available presence data. Each dot is the average of at least five predictions corresponding to the 5 general circulation models, multiplied by the number of species with such sample size (see Appendix 4 for details of sample size per species).

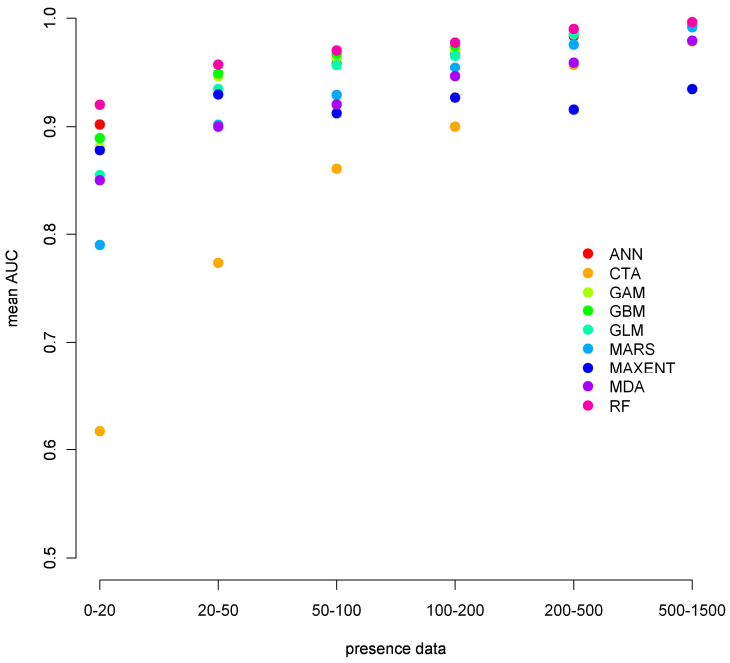

Figure S4. Distribution of the log-ratio of predicted future and present range sizes according to the climate suitability model used.

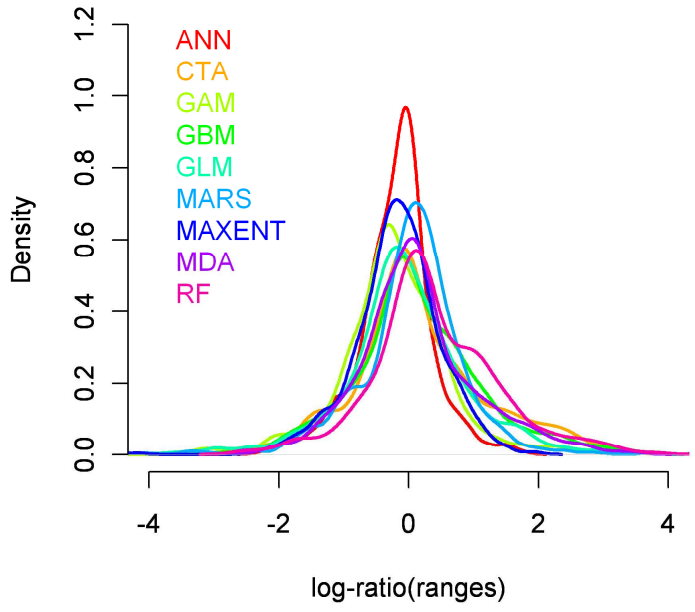

An important issue regarding niche modelling is the variability of results when using different modelling techniques (Araújo *et al*. 2005; Thuiller 2004; Pearson *et al*. 2006; Thuiller *et al*. 2004). Uncertainty can also ensue from variability in climate change projections (Appendix 5). Nevertheless, the use of ensemble forecast techniques seems to be a good way of reducing these problems (Araújo *et al*. 2005; Thuiller *et al*. 2005). Therefore, in this study 9 different modelling tools were used, and the variability across their performances is another good example showing the importance of not considering only one model (see the case of the SRE model, similar to the well-known BioClim model). The use of a consensus method considering the 5 best models out of the 9 used shows that the best performing models are not always the same for different species, even if some of them (RF, GBM, GAM, ANN and GLM) generally perform better. The performance also varies according to the species under study and the number of available presence records, corroborating results of other studies (Elith *et al*. 2006) and highlighting the importance and relevance of using several modelling tools (Araújo & New 2007).

Araújo, M.B. & New, M. 2007 Ensemble forecasting of species distributions. *Trends Ecol. Evol.* **22**, 42-47.

Araújo, M.B., Whittaker, R.J., Ladle, R.J. & Erhard, M. 2005 Reducing uncertainty in projections of extinction risk from climate change. *Global Ecol. Biogeogr.* **14**, 529-538.

Breiman, L., Friedman, J.H., Olshen, R.A., *et al.* 1984 Classification and Regression Trees. Chapman & Hall, New York.

Breiman, L. 2001 Random Forests. *Mach. Learn.* **45**, 5-32.

Elith, J., Graham, C.H., Anderson, R.P., Dudík, M., Ferrier, S., Guisan, A., Hijmans, R.J., Huettmann, F., Leathwick, J.R., Lehmann, A., *et al*. 2006. Novel methods improve prediction of species' distributions from occurrence data. *Ecography* **29**, 129-151.

Fielding, A.H. & Bell, J.F. 1997 A review of methods for the assessment of prediction errors in conservation presence/ absence models. *Environmental Conservation* **24**,:38-49.

Friedman, J. 1991 Multivariate adaptive regression splines (with discussion). *Ann. Stat*. **19**, 1-141.

Hastie, T. & Tibshirani, R. 1996 Discriminant Analysis by Gaussian Mixtures. *Journal of the Royal Statistical Society Series B – Methodological* **58**,155-176.

Keith, S., Fry, C. *et al*. 1992-2004. *The birds of Africa: Vol 4-7*. Academic Press, London.

Lobo, J.M., Jiménez-Valverde, A. & Real, J. 2008. AUC: misleading measure of the performance of predictive distribution models. Global Ecol Biogeogr. **17:** 145-151.

Pearson, R.G., Thuiller, W., Araújo, M.B., Martinez-Meyer, E., Brotons, L., McClean, C., Miles, L., Segurado, P., Dawson, T.P. & Lees, D.C. 2006 Model-based uncertainty in species range prediction. *J. Biogeogr.* **33**, 1704-1711.

Phillips, S.J., Anderson, R.P. & Schapire, R.E. 2006 Maximum entropy modeling of species geographic distributions. *Ecol. Model*. **190**,231–259.

Ridgeway, G. 1999 The state of boosting. *Computing Science and Statistics* **31**, 172-181.

Ripley, B.D. 1996 Pattern recognition and neural networks. Cambridge University Press, Cambridge.

Swets, J.A. 1988 Measuring the accuracy of diagnostic systems. *Science* **240**, 1285-1293.

Thuiller, W. 2003 BIOMOD – optimizing predictions of species distributions and projecting potential future shifts under global change. *Global Change Biol*. **9**, 1353-1362.

Thuiller, W. 2004 Patterns and uncertainties of species' range shifts under climate change. *Global Change Biol*. **10**, 2020–2027.

Thuiller, W., Araújo, M.B., Pearson, R.G., Whittaker, R.J., Brotons, L. & Lavorel, S. 2004 Biodiversity conservation: uncertainty in predictions of extinction risk. *Nature* **430**, 33.

Thuiller, W., Lavorel, S., Araújo, M.B., Sykes, M.T. & Prentice, I.C. 2005 Climate change threats to plant diversity in Europe. *Proc. Natl. Acad. Sci. USA*, **102**, 8245-8250.

Appendix 2. Assessing the effects of pseudo-absences and choice of the method

We aimed at testing the robustness of the modelled distributions depending on how we defined pseudo-absences, in order to decide which method was more appropriate. We tested 2 different methods for creating pseudo-absences. For both methods, the total number of presences and pseudo-absences was fixed to 2000, which is one sixth of the total considered area. We thus consider that a species recorded in many pixels of the study area would certainly be absent from a small number of pixels across the rest of Africa (because it is a 'common' species with a widespread distribution), whereas a species with a small sample size is more likely to be absent from most of Africa, because it has not been recorded widely. The parameter we tested was the way of creating the pseudo-absences, which are either picked randomly in any points where the species was not recorded or in the area considered unsuitable for the species according to the surface range envelop (Le Maître *et al*., 2008) model. SRE (Busby 1991) is an envelope-style method that characterizes sites that are located within the environmental hyper-space occupied by a species. For both methods, the analysis was fully conducted as previously described. In order to compare the accuracy of the modelled distributions, we tested for a difference in the mean AUC of the models selected for a species. We also look for a difference in AUC calculated from the independent set of data digitized from the volumes of "The Birds of Africa" series (Keith & Fry 1992-2004).

There was no significant difference between the independent AUC (paired t-test, $t=1.68$, $df=62$, $p=0.098$). However, regarding the mean AUC calculated from our data of the selected models, the modelled distributions obtained when picking the pseudo-absences randomly out of the SRE model turned out to be more accurate (paired t-test, $t=-4.89$, $df=63$, $p<0.001$). Therefore, the results presented in the study are those obtained when using the SRE model to choose the pseudo-absences.

Busby, J.R. 1991 BIOCLIM - a bioclimate analysis and prediction system. In: Margules, C. R. and Austin, M. P. (eds), *Nature conservation: cost effective biological surveys and data analysis*. CSIRO, pp. 64-68.

Keith, S., Fry, C. *et al*. 1992-2004. *The birds of Africa: Vol 4-7*. Academic Press, London.

Le Maître, D.C., Thuiller, W. & Schonegevel, L. 2008. Developing an approach to defining the potential distributions of invasive plant species: a case study of Hakea species in South Africa. *Global Ecol. Biogeogr*. **17**, 569-584. (doi: 10.1111/j.1466-8238.2008.00407.x)

Appendix 3. Model accuracy: average ± standard error of AUC values obtained for each species when predicting the present distribution of climate suitability, considering all modelling techniques (first column) or only the 5 retained in the ensemble forecast framework (second column). The fifth column presents AUC calculated from an independent set of data (as described in Appendix 1), the last two columns providing the sensitivity and the specificity related.

Latin name	English name	AUC, all models	AUC, ensemble forecast models	AUC (independent data)	Sensitivity	Specificity
Acrocephalus arundinaceus	Great Reed Warbler	0.974 ± 0.024	0.990 ± 0.003	0.942	0.841	0.865
Acrocephalus griseldis	Basra Reed Warbler	0.935 ± 0.050	0.963 ± 0.011	0.990	0.857	0.974
Acrocephalus paludicola	Aquatic Warbler	0.827 ± 0.147	0.920 ± 0.043	-	-	-
Acrocephalus palustris	Marsh Warbler	0.970 ± 0.023	0.981 ± 0.005	0.952	0.588	0.966
Acrocephalus schoenobaenus	Sedge Warbler	0.970 ± 0.028	0.988 ± 0.004	0.933	0.797	0.892
Acrocephalus scirpaceus	European Reed Warbler	0.912 ± 0.062	0.955 ± 0.010	0.909	0.838	0.829
Anthus campestris	Tawny Pipit	0.935 ± 0.036	0.960 ± 0.012	0.930	0.644	0.959
Anthus cervinus	Red-throated Pipit	0.921 ± 0.041	0.953 ± 0.017	0.876	0.537	0.883
Anthus trivialis	Tree Pipit	0.941 ± 0.042	0.970 ± 0.006	0.941	0.757	0.916
Calandrella brachydactyla	Short-toed Lark	0.907 ± 0.066	0.948 ± 0.018	0.847	0.256	0.981
Delichon urbicum	House Martin	0.980 ± 0.016	0.990 ± 0.003	0.909	0.543	0.942
Emberiza caesia	Cretzsmar's Bunting	0.900 ± 0.089	0.952 ± 0.025	0.983	0.707	0.988
Emberiza hortulana	Ortolan Bunting	0.880 ± 0.095	0.935 ± 0.029	0.873	0.371	0.979
Ficedula albicollis	Collared Flycatcher	0.950 ± 0.049	0.972 ± 0.009	0.932	0.572	0.969
Ficedula hypoleuca	Pied Flycatcher	0.918 ± 0.054	0.954 ± 0.020	0.966	0.683	0.971
Ficedula semitorquata	Semi-collared Flycatcher	0.926 ± 0.088	0.971 ± 0.022	0.988	0.551	0.992
Hippolais icterina	Icterine Warbler	0.982 ± 0.012	0.991 ± 0.003	0.953	0.581	0.968
Hippolais languida	Upcher's Warbler	0.947 ± 0.048	0.969 ± 0.008	0.985	0.785	0.975
Hippolais olivetorum	Olive-tree Warbler	0.958 ± 0.030	0.975 ± 0.010	0.978	0.877	0.946
Hippolais polyglotta	Melodious Warbler	0.915 ± 0.055	0.949 ± 0.020	0.988	0.734	0.993
Hirundo rustica	Swallow	0.757 ± 0.130	0.840 ± 0.054	0.998	0.947	0.896
Irania gutturalis	White-throated Robin	0.980 ± 0.028	0.994 ± 0.003	0.983	1.000	0.972
Lanius collurio	Red-backed Shrike	0.917 ± 0.087	0.959 ± 0.019	0.998	0.923	0.884
Lanius isabellinus	Isabelline Shrike	0.987 ± 0.017	0.996 ± 0.001	0.972	0.370	0.971
Lanius minor	Lesser Grey Shrike	0.933 ± 0.028	0.951 ± 0.012	0.886	0.985	0.938
Lanius nubicus	Masked Shrike	0.987 ± 0.011	0.994 ± 0.003	0.993	0.822	0.874

Lanius senator	Woodchat Shrike	0.942 ± 0.050	0.973 ± 0.006	0.903	0.808	0.820
Locustella fluviatilis	River Warbler	0.930 ± 0.055	0.968 ± 0.016	0.914	0.966	0.948
Locustella luscinioides	Savi's Warbler	0.919 ± 0.046	0.949 ± 0.017	0.989	0.584	0.901
Locustella naevia	Grasshopper Warbler	0.881 ± 0.102	0.938 ± 0.036	0.885	0.288	0.986
Luscinia luscinia	Thrush Nightingale	0.787 ± 0.089	0.840 ± 0.064	0.908	0.878	0.965
Luscinia megarhynchos	Nightingale	0.962 ± 0.036	0.981 ± 0.006	0.985	0.740	0.879
Luscinia svecica	Bluethroat	0.940 ± 0.039	0.966 ± 0.012	0.922	0.495	0.969
Melanocorypha bimaculata	Bimaculated Lark	0.871 ± 0.084	0.926 ± 0.029	0.896	0.343	1.000
Monticola saxatilis	Rock Thrush	0.855 ± 0.158	0.949 ± 0.070	0.986	0.811	0.734
Monticola solitarius	Blue Rock Thrush	0.942 ± 0.024	0.959 ± 0.013	0.839	0.389	0.915
Motacilla alba	White Wagtail	0.904 ± 0.067	0.944 ± 0.022	0.745	0.475	0.940
Motacilla cinerea	Grey Wagtail	0.817 ± 0.074	0.925 ± 0.022	0.851	0.823	0.888
Motacilla flava	Yellow Wagtail	0.930 ± 0.034	0.954 ± 0.016	0.922	0.945	0.914
Muscicapa striata	Spotted Flycatcher	0.962 ± 0.038	0.985 ± 0.005	0.970	0.974	0.913
Oenanthe deserti	Desert Wheatear	0.983 ± 0.022	0.995 ± 0.002	0.979	0.253	0.936
Oenanthe hispanica	Black-eared Wheatear	0.938 ± 0.040	0.960 ± 0.007	0.739	0.522	0.949
Oenanthe isabellina	Isabelline Wheatear	0.917 ± 0.054	0.953 ± 0.014	0.917	0.493	0.938
Oenanthe oenanthe	Common Wheatear	0.956 ± 0.025	0.970 ± 0.008	0.818	0.474	0.827
Oenanthe pleschanka	Pied Wheatear	0.949 ± 0.032	0.971 ± 0.008	0.776	0.596	0.982
Oenanthe xanthoprymna	Kurdish Wheatear	0.952 ± 0.040	0.972 ± 0.007	0.967	0.117	1.000
Oriolus oriolus	Golden Oriole	0.890 ± 0.145	0.984 ± 0.020	0.944	0.695	0.900
Phoenicurus phoenicurus	Common Redstart	0.979 ± 0.018	0.990 ± 0.004	0.934	0.665	0.925
Phylloscopus bonelli	Bonelli's Warbler	0.941 ± 0.035	0.964 ± 0.008	0.933	0.633	0.989
Phylloscopus collybita	Chiffchaff	0.947 ± 0.048	0.972 ± 0.014	0.979	0.417	0.933
Phylloscopus sibilatrix	Wood Warbler	0.941 ± 0.042	0.967 ± 0.013	0.722	0.992	0.833
Phylloscopus trochilus	Willow Warbler	0.937 ± 0.049	0.977 ± 0.011	0.973	0.952	0.894
Ptyonoprogne rupestris	Crag Martin	0.984 ± 0.023	0.896 ± 0.001	0.973	1.000	0.991
Riparia riparia	Sand Martin	0.963 ± 0.023	0.981 ± 0.005	0.858	0.619	0.831
Saxicola rubetra	Whinchat	0.943 ± 0.042	0.969 ± 0.016	0.921	0.844	0.853
Sylvia atricapilla	Blackcap	0.916 ± 0.049	0.949 ± 0.014	0.864	0.590	0.856
Sylvia borin	Garden Warbler	0.971 ± 0.032	0.989 ± 0.004	0.937	0.929	0.797
Sylvia cantillans	Subalpine Warbler	0.928 ± 0.063	0.965 ± 0.013	0.963	0.673	0.976
Sylvia communis	Common Whitethroat	0.959 ± 0.027	0.977 ± 0.008	0.916	0.756	0.888
Sylvia curruca	Lesser Whitethroat	0.909 ± 0.075	0.949 ± 0.015	0.870	0.395	0.959
Sylvia hortensis	Orphean Warbler	0.921 ± 0.066	0.960 ± 0.020	0.914	0.532	0.957
Sylvia mystacea	Menetries' Warbler	0.880 ± 0.067	0.916 ± 0.035	0.922	0.741	0.977

Sylvia nisoria	Barred Warbler	0.934 ± 0.052	0.962 ± 0.017	0.990	0.870	0.974
Sylvia rueppelli	Ruppell's Warbler	0.940 ± 0.063	0.972 ± 0.010	0.948	0.702	0.987

Appendix 4. The following table gives, for each studied species (n = 64), the sample size of the presence data, the size of the predicted present range, the ratio between the future and the present ranges, the overlap between these two ranges as a proportion of the predicted present range, and the potential range shift (in km) as the distance between centroids of predicted present and future ranges. Even though an increase of the geographical range is not possible with the no-dispersal hypothesis, range overlaps > 1 occur as range sizes were estimated using indices calculated with suitability probabilities.

Species	Presence data	Present range size ($\times 10^4$ km^2)	Ratio of range sizes	Range overlap	Range shift (km)
Acrocephalus arundinaceus	278	3608	0,88	0,81	327
Acrocephalus griseldis	41	145	0,66	0,52	315
Acrocephalus paludicola	10	108	8,53	1,29	1397
Acrocephalus palustris	165	567	0,31	0,30	672
Acrocephalus schoenobaenus	237	3773	0,79	0,71	313
Acrocephalus scirpaceus	65	2281	1,05	0,97	200
Anthus campestris	64	721	1,41	0,96	472
Anthus cervinus	56	930	1,62	1,09	193
Anthus trivialis	102	1753	0,81	0,70	339
Calandrella brachydactyla	35	229	4,20	1,45	1188
Delichon urbicum	497	2438	0,50	0,49	165
Emberiza caesia	23	105	5,17	0,94	553
Emberiza hortulana	20	147	0,27	0,18	1413
Ficedula albicollis	44	366	0,03	0,03	509
Ficedula hypoleuca	39	484	2,70	1,23	1201
Ficedula semitorquata	16	148	0,03	0,03	655
Hippolais icterina	347	1249	0,23	0,22	698
Hippolais languida	55	256	0,62	0,50	91
Hippolais olivetorum	71	495	0,33	0,24	657
Hippolais polyglotta	27	331	2,85	1,12	1283
Hirundo rustica	1201	5568	0,50	0,50	252
Irania gutturalis	39	212	0,22	0,22	68
Lanius collurio	758	2757	0,18	0,18	631
Lanius isabellinus	58	399	0,69	0,55	163
Lanius minor	598	1395	0,21	0,21	717
Lanius nubicus	90	1005	1,92	1,11	624
Lanius senator	71	1715	1,56	1,20	173
Locustella fluviatilis	35	503	0,34	0,31	410
Locustella luscinioides	29	605	2,71	1,38	889
Locustella naevia	15	79	10,82	0,99	544
Luscinia luscinia	103	598	0,08	0,06	287

Luscinia megarhynchos	50	1155	1,18	1,00	127
Luscinia svecica	24	402	0,94	0,69	502
Melanocorypha bimaculata	6	23	5,85	0,97	1152
Monticola saxatilis	116	2024	0,77	0,73	512
Monticola solitarius	36	444	1,49	0,70	1359
Motacilla alba	36	557	2,22	1,10	280
Motacilla cinerea	80	660	1,43	0,79	745
Motacilla flava	269	5283	0,85	0,85	96
Muscicapa striata	824	4556	0,42	0,42	191
Oenanthe deserti	53	434	1,61	1,04	113
Oenanthe hispanica	43	425	1,56	1,05	72
Oenanthe isabellina	133	871	0,57	0,51	316
Oenanthe oenanthe	103	1587	1,29	0,92	57
Oenanthe pleschanka	90	382	0,92	0,66	446
Oenanthe xanthoprymna	6	9	0,51	0,13	200
Oriolus oriolus	449	2627	0,20	0,20	463
Phoenicurus phoenicurus	75	879	0,74	0,43	806
Phylloscopus bonelli	34	327	2,43	1,32	325
Phylloscopus collybita	65	798	0,85	0,53	793
Phylloscopus sibilatrix	53	1999	1,40	1,14	256
Phylloscopus trochilus	806	5119	0,61	0,61	158
Ptyonoprogne rupestris	10	42	3,96	0,82	267
Riparia riparia	253	2562	0,62	0,56	359
Saxicola rubetra	75	1549	0,86	0,78	136
Sylvia atricapilla	50	899	0,94	0,79	159
Sylvia borin	323	4199	0,84	0,75	521
Sylvia cantillans	41	419	1,97	1,24	328
Sylvia communis	213	2273	0,89	0,79	475
Sylvia curruca	35	369	1,05	0,63	730
Sylvia hortensis	29	350	2,89	1,46	711
Sylvia mystacea	23	141	2,83	0,84	1401
Sylvia nisoria	33	232	0,49	0,48	175
Sylvia rueppelli	28	174	0,22	0,20	382

Appendix 5. Climate models and climate scenarios variability

The distribution of one of our impact estimate according to general circulation models and SRES climate scenarios indicates that average values are similar, but distribution tails are different. Therefore the different general circulation models and SRES scenarios did not influence the average changes in range size, but influenced the intensity of the increases or decreases in range. Predictions obtained with the BCM2 and MK3 models showed a less important effect of the climate change over the wintering ranges variations (Figure S5). Scenario A2 makes predictions with larger variations than the A1 scenario, the A1 scenario itself giving larger variations than the B1 scenario (Figure S6). Nevertheless, this variability regarding climate models and scenarios underlines the importance of taking these ensembles into account, in order to improve the predictions accuracy. IPCC SRES scenarios A1, A2 and B1 reflect the potential impact of different assumptions about demographic, socio-economic and technological development on the release of greenhouse gases. The A1 scenario describes a globalized world with rapid economic growth and global population that peaks in mid-century and declines thereafter, and it assumes a rapid introduction of new and more efficient technologies. The A2 scenario describes a heterogeneous world with regionally oriented economic development. Per capita economic growth and technological change are slower than in the other scenarios. The B1 scenario describes a convergent world with global population that peaks in mid-century and declines thereafter, as in A1, but with a rapid change toward a service and information economy and the introduction of clean and resource-efficient technology.

It can also be interesting to focus on the variance of our impact estimates across the GCMs for each species, because current GCMs show little agreement on patterns of rainfall change, particularly in sub-Saharan Africa. For every species and every GCM, the mean value of the shift, the ratio of range sizes and the range overlap was calculated, considering the different scenarios and the selected models. Figure S7 shows the correlation between the mean and the standard deviation across GCMs for the 3 impact estimates, each dot standing for a species. For each of the estimates, the variance increases with the mean. The average ratio between the standard deviation and the mean is 17% (range 5-39%) for the shift, 22% (range 1-62%) for the ratio of range sizes and 18% (range 2-66%) for the range overlap. Therefore, for some species the variance of the GCMs can lead to an important variance across the projected distributions. Nevertheless this uncertainty can only decrease with the

improvement of the GCMs, and underlines the importance of the ensemble forecast technique considering several GCMs to obtain the central tendency.

Figure S5. Distribution of the log-ratio between predicted present and future range sizes according to the general circulation models.

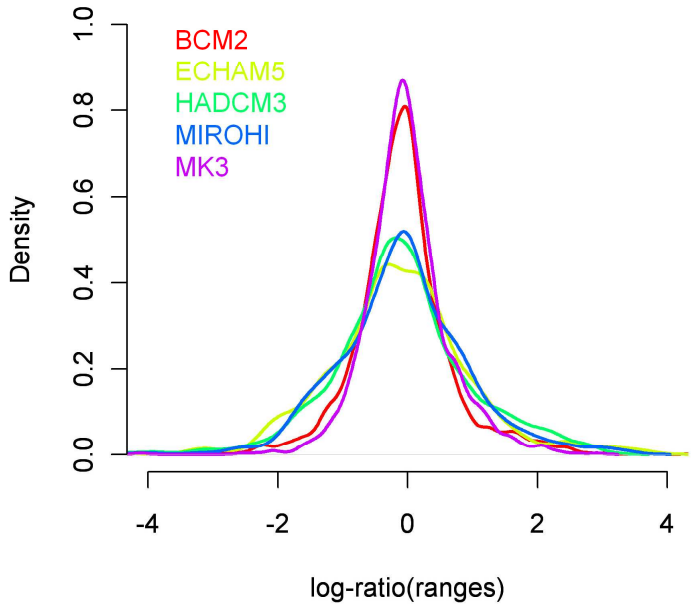

Figure S6. Distribution of the log-ratio between predicted present and future range sizes according to the S

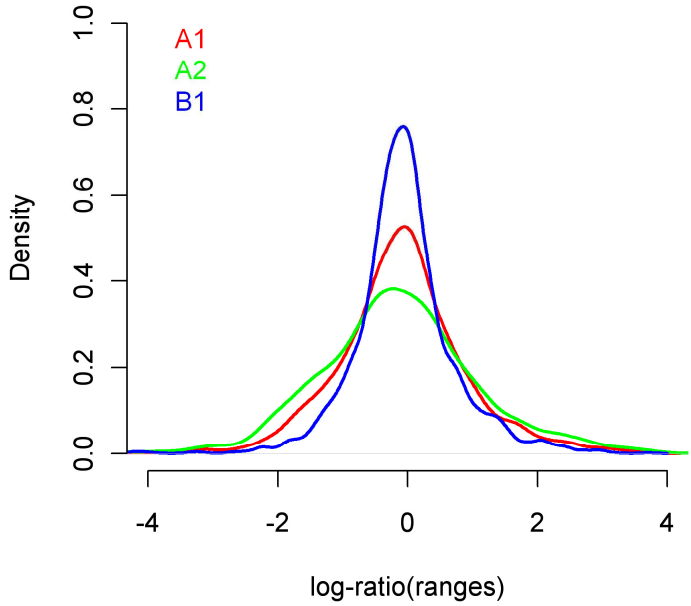

Figure S7. Relationships between the mean and the standard deviation of (a) the predicted shift in distribution, (b) the ratio of range sizes and (c) the range overlap across the 5 GCMs values for each species.

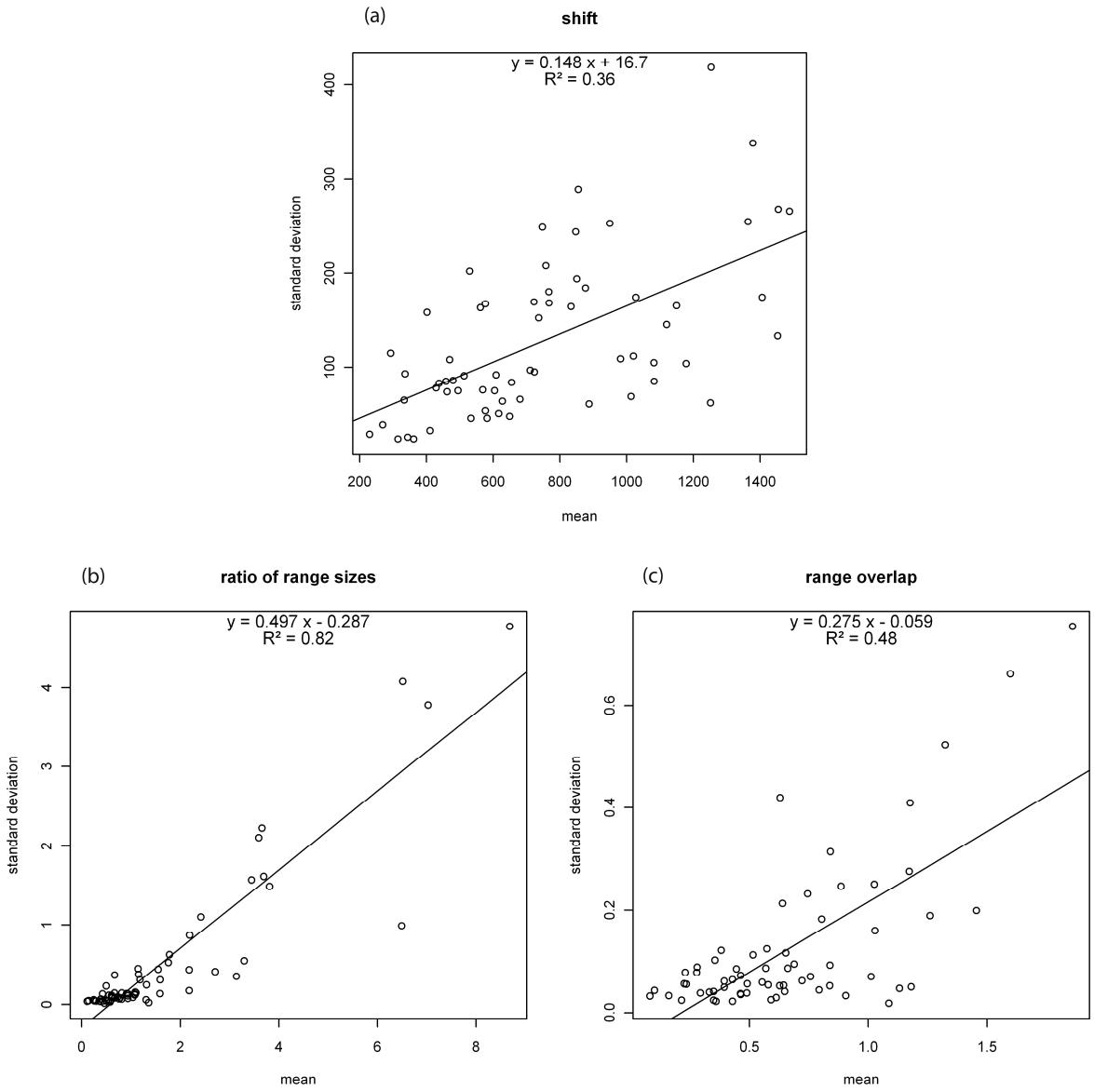

Appendix 6. Trends analysis and phylogenetic non-independence of species

Species are more or less phylogenetically related. Hence, the species studied might not represent independent points in statistical analyses, and results of linear models could be biased if not accounting for phylogenetic relatedness among species. Closely related species have a common evolutionary history, and niche conservatism in evolutionary times is often reported (e.g. Peterson *et al.* 1999), so multi-species statistical analyses on niche changes should consider potential phylogenetic biases. On the other hand, because closely related species tend to compete between each other, their distribution and niche breadth should show a greater difference than expected by chance. A correction for phylogenetic relatedness was considered in the models we performed to explain our three variables estimating potential impacts of climate change on winter ranges (change in range size, range overlap and range shift) by the initial location and size of the present predicted range. We used the Generalized Least Squares phylogenetic comparative method (Martins *et al.* 2002, Freckleton *et al.* 2002), with the 'ape' package of the R-software. We computed the phylogenetic tree of the species using the classification published by Jønsson & Fjeldså (2006) (see Figure S8 below for details), with the assumption that all branches in the phylogeny are of equal length. We ran GLSs with a model dependence linked to the phylogenetic tree assuming a Grafen correlation structure (as no branch lengths were available; Grafen's method uses a Brownian approach but estimates branch lengths from the data). Results of these models are presented in Table 1 included in the main text of the paper. Weighted Linear Models, without considering a phylogenetic correction, produced almost similar results.

Aliabadian, M., Kaboli, M., Prodon, R., Nijman, V. & Vences, M. 2007 Phylogeny of Palaearctic wheatears (genus *Oenanthe*) – Congruence between morphometric and molecular data. *Mol. Phyl. Evol.* **42**, 665-675. (doi:10.1016/j.ympev.2006.08.018)

Freckleton, R. P., Harvey, P. H. & Pagel, M. 2002 Phylogenetic analysis and comparative data: a test and review of evidence. *Am. Nat.* **160**, 712-726. (doi:0003-0147/2002/16006-010368$15.00)

Jønsson, K. A. & Fjeldså, J. 2006 A phylogenetic supertree of oscine passerine birds (Aves: Passeri). *Zoologica Scripta* **35**, 149-186.

Martins, E. P., Diniz-Filho, J. A. F. & Housworth, E. A. 2002 Adaptive constraints and the phylogenetic comparative method: a computer simulation test. *Evolution* **56**, 1-13 (doi: 10.1043/0014-3820(2002)056<0001:ACATPC>2.0.CO;2)

Mundy, N.I. & Helbig, A.J. 2004 Origin and Evolution of Tandem Repeats in the Mitochondrial DNA Control Region of Shrikes (*Lanius spp*.). *J. Mol. Evol.* **59**, 250-257. (doi:10.1007/s00239-004-2619-6)

Peterson, A.T., Soberón, J. & Sánchez-Cordero, V. 1999 Conservatism of ecological niches in evolutionary time. *Science* **285**, 1265-1267. (doi:10.1126/science.285.5431.1265)

Wei, Z., Fu-Min, L., Gang, L., Zuo-Hua, Y., Hong-Feng, Z., Hong-Jian, W. & Anton, K. (2007) *Acta Ornithologica* **42**, 173-180. (doi:10.3161/000164507783516863)

Figure S8. Phylogenetic tree of the 64 studied bird species. The classification published by Jønsson & Fjeldså (2006) was used, with a few adaptations using: Aliabadian *et al.* (2007) for the *Oenanthe* wheatears, Wei *et al.* (2007) and Mundy & Helbig (2004) for the *Lanius* shrikes. No published phylogenetic study was available to place the White-throated Robin (*Irania gutturalis*) on the tree, so it was arbitrarily placed close to *Phoenicurus phoenicurus* because of common taxonomic knowledge.

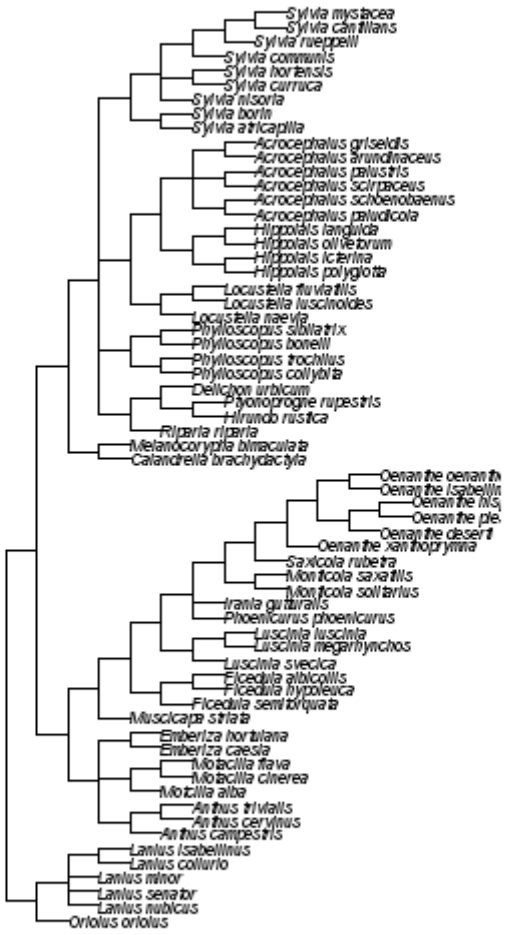

Appendix 7. Barplots of the distribution of predicted changes in range size for the 64 species according to the three time intervals considered in the study. The first graph (a) considers that species would be able to disperse fully from predicted present range to predicted future range. The second graph (b) considers that species would not disperse and would occupy only the overlap between the two ranges. Even though an increase of the geographical range is not possible with the no-dispersal hypothesis, range overlaps > 1 occur as range sizes were estimated using indices calculated with suitability probabilities.

(a)

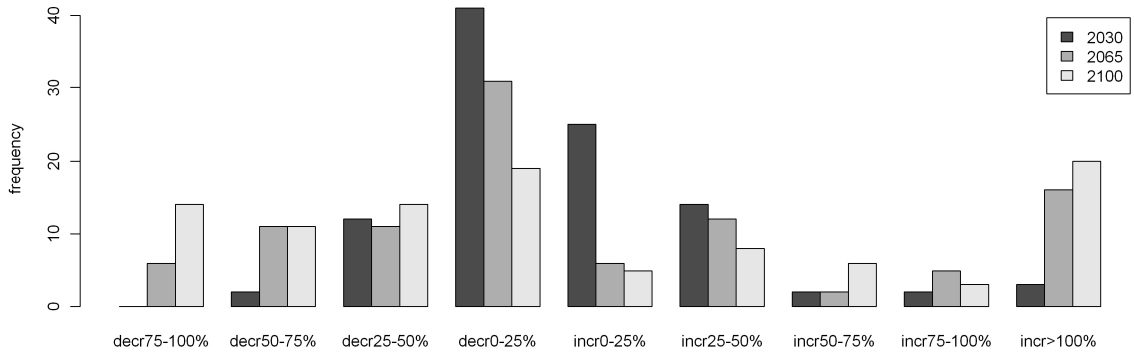

(b)

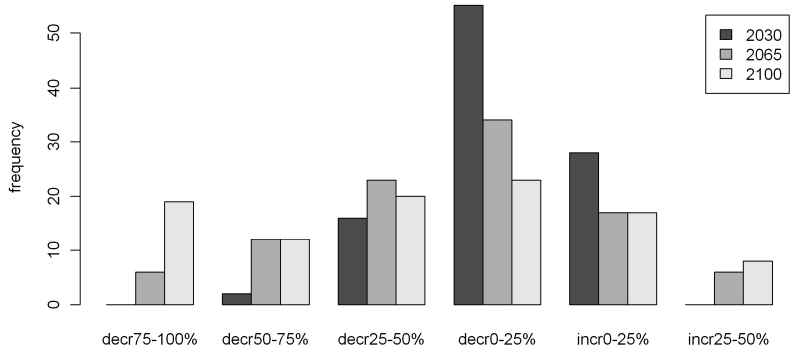

Appendix 8. Examples of output maps for a sample of species

We present here different graphic outputs for three closely related species, the *Ficedula* flycatchers. For two of them, we predicted the largest range reductions (97%) and the smallest range overlaps (3%) between modelled present and future ranges. For all species, the first map represents the species winter range as published in the "The Birds of Africa" series (Keith *et al.* 1992-2004), including both core winter range and marginal areas. The red open dots indicate the record localities used in our models. Below this map, the four maps on the left present the predicted ranges obtained using the ensemble forecast framework and using the present and the three future climate projections data (for time intervals 1961-1990, 2011-2030, 2046-2065 and 2080-2099), showing pixels with probability of suitability when the latter was above the retained threshold, the black pixel representing the centroid. The four maps on the right present the corresponding standard error of probabilites, as the unweighted standard error of the 25 (present) or 60 (future) distributions used in the consensus approach. Standard errors are shown without excluding probabilities below the retained threshold.

Keith, S., Fry, C. *et al*. 1992-2004. *The birds of Africa: Vol 4-7*. Academic Press, London.

Figure S9. Output maps for the Collared Flycatcher *Ficedula albicollis*.

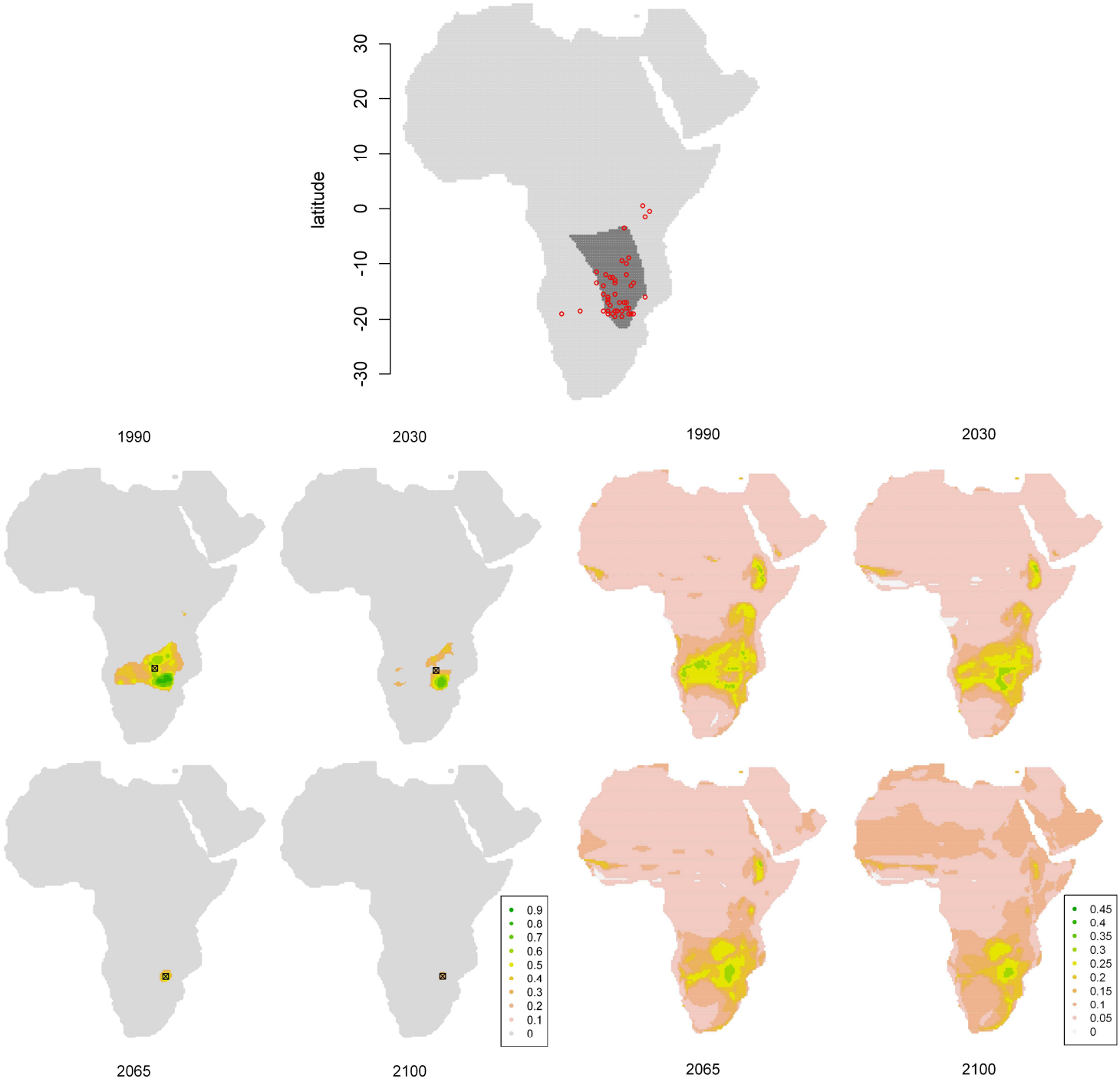

Figure S10. Output maps for the Pied Flycatcher *Ficedula hypoleuca*.

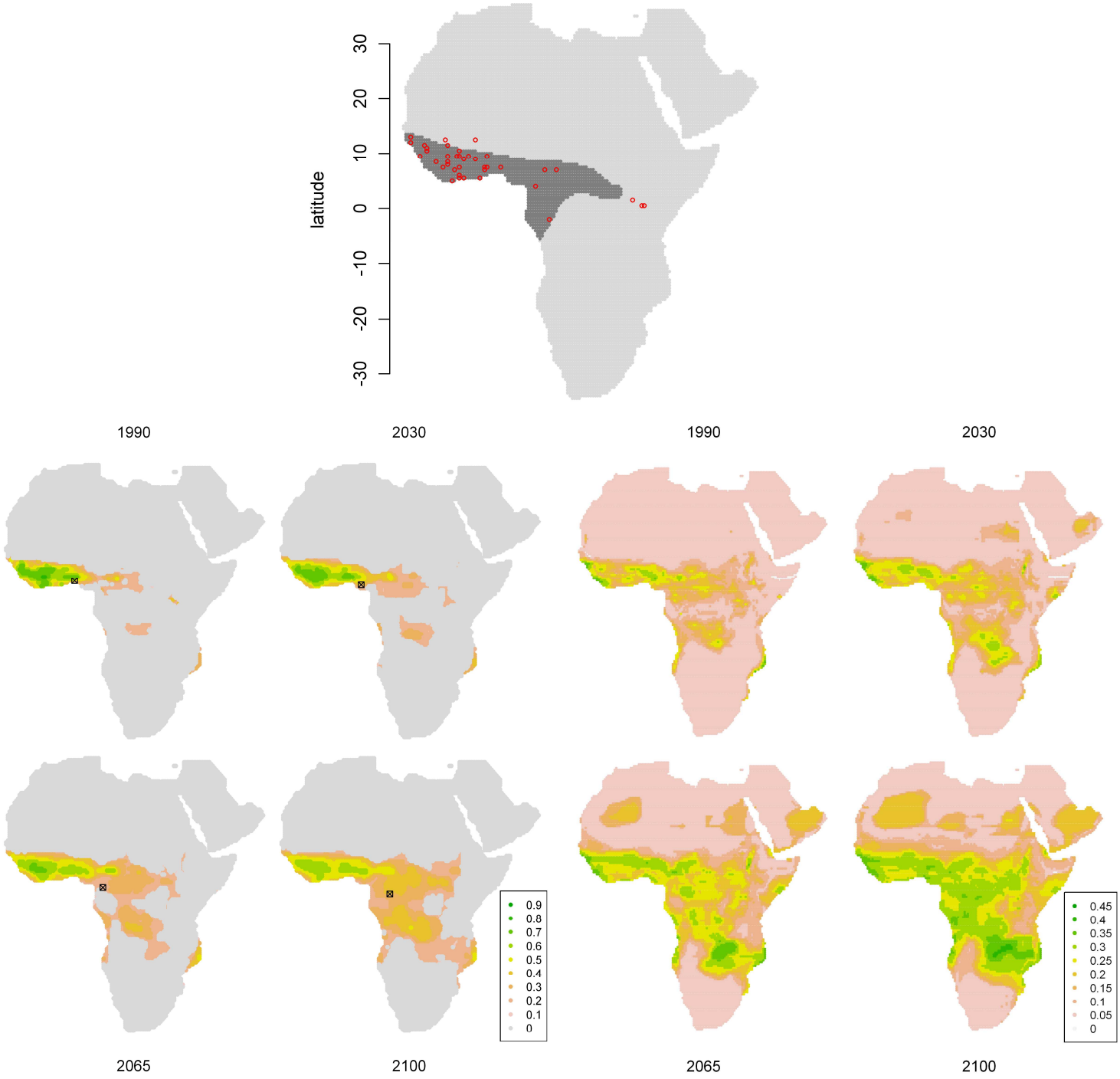

Figure S11. Output maps for the Semi-collared Flycatcher *Ficedula semitorquata*.